Progress In Electromagnetics Research M, Vol. 104, 13–22, 2021

Analysis of Novel Eddy Current Damper for Multi-Ring Permanent Magnet Thrust Bearing

Dhruv Deshwal[1], Siddappa I. Bekinal[1, *], and Mrityunjay Doddamani[2]

Abstract—This paper deals with analyzing a novel eddy current damper for an axially magnetized multi-ring permanent magnet thrust bearing (MPMTB). Initially, the bearing is optimized for maximum axial force by selecting three general parameters (air gap, outer diameter of stator, and length) using a generalized optimization procedure. Then, the axial force of an optimized bearing is validated with the mathematical model results. Finally, the novel and conventional eddy current dampers (ECDs) for an optimized MPMTB are analyzed for damping forces and coefficients using three-dimensional (3D) finite element transient analysis in ANSYS. Based on the analysis results, the proposed novel structure could be selected to replace the conventional one for providing damping to MPMTB effectively without affecting the radial air gap between the rotor and stator rings.

1. INTRODUCTION

Permanent magnet bearings (PMBs) [1] are simple and robust in construction as compared to active magnetic bearings [2]. These are realized only with the permanent magnets without any sensors, actuators, and feedback control systems. In many applications [3–6], PMBs have replaced conventional bearings to increase system efficiency. Design equations for force and stiffness in monolithic [7–12], as well as multi-ring PMB [13–16], were presented by many researchers using Amperian or Coulombian models. Optimization [17–20] of different parameters of PMB was carried out to enhance the values of bearing characteristics. Despite attractive features, PMB is associated with instability and poor damping characteristics. The instability issue was addressed by the researchers using PMB in combination with either active or superconducting magnetic bearings. The damping characteristic of PMB can be enhanced by active [21] or passive means. Active dampers impose electronic equipment and require external energy sources, whereas passive dampers such as viscoelastic [22] and eddy current do not need any sensors and energy sources. Non-contact ECDs are the best possible choice for improving the damping property of PMBs. In an axially magnetized monolithic PMB, authors [23] provided a copper material on the rotor to form an ECD and developed 3D equations for damping force and coefficients. A greater deviation of results of 3D equations from experiments was noticed. Fang et al. [24] proposed an eddy current damping system for a high-speed turbo compressor rotor. They presented a mathematical model and optimal design procedure for maximizing axial stiffness and improving the damping coefficient. Detoni et al. [25] presented a mathematical model for identifying ECD characteristics for PMB-supported rotors. The presented analytical model was used along with the curve fitting results of FEA for evaluating the parameters associated with mechanical impedance. In [26], the authors presented a two-dimensional analytical model for calculating damping coefficients in a compact PMB consisting of Halbach arrays and ECD. Results of analytical equations were verified with

Received 1 July 2021, Accepted 26 July 2021, Scheduled 2 August 2021

* Corresponding author: Siddappa I. Bekinal (siddappabekinal@gmail.com).

[1] Department of Mechanical and Manufacturing Engineering, Manipal Institute of Technology, Manipal Academy of Higher Education, Manipal, Udupi, Karnataka 576104, India. [2] Department of Mechanical Engineering, National Institute of Technology Karnataka, Surathkal, Mangalore, Karnataka 575025, India.

3D FEA results. In the research efforts on ECD development to PMB, authors included the conductor plate in the radial air gap (i.e., on the stator or rotor rings). This leads to a smaller radial air gap and affects the characteristics of PMB. In addition, it was shown in the literature [27, 28] that an air gap between the axial stacks of axially polarized MPMTB enhances force values. There exists an optimum value of an axial air gap at which force is optimum compared to bearing without an axial air gap. In our earlier efforts [29], a generalized optimization procedure for axially polarized multi-ring thrust and radial PMB with an air gap between axial stacks was presented. In the present work, copper rings are considered in the axial air gaps of the rotor rings to present the novel eddy current damper concept to PMB. The contributions of this paper are (i) the optimization of axially magnetized multi-ring PMB by selecting radial air gap, outer diameter of stator and length of a bearing using generalized optimization procedure, (ii) validation of force results of MPMTB obtained using generalized optimization procedure and mathematical model, and (iii) analysis of novel and conventional eddy current dampers for axial and radial damping forces and coefficients using 3D FEA transient analysis.

2. BEARING CONFIGURATIONS WITH EDDY CURRENT DAMPER

The permanent magnet thrust bearing is realized by providing one ring on the rotor and the other on the stator with the polarization directions (axial) opposite to one another as shown in Fig. 1(a). As compared to conventional bearings, the force and stiffness values generated in such a monolithic bearing are low. This issue can be resolved by providing multi-rings on the stator and rotor to form MPMTB. An air gap can also be provided between the adjacent rings of both stator and rotor to improve bearing characteristics. Axially polarized MPMTB with a copper plate on the rotor to form an ECD (configuration I) is shown in Fig. 1(b) and with copper rings in the axial air gaps of the rotor rings to form a novel ECD (configuration II) as shown in Fig. 1(c).

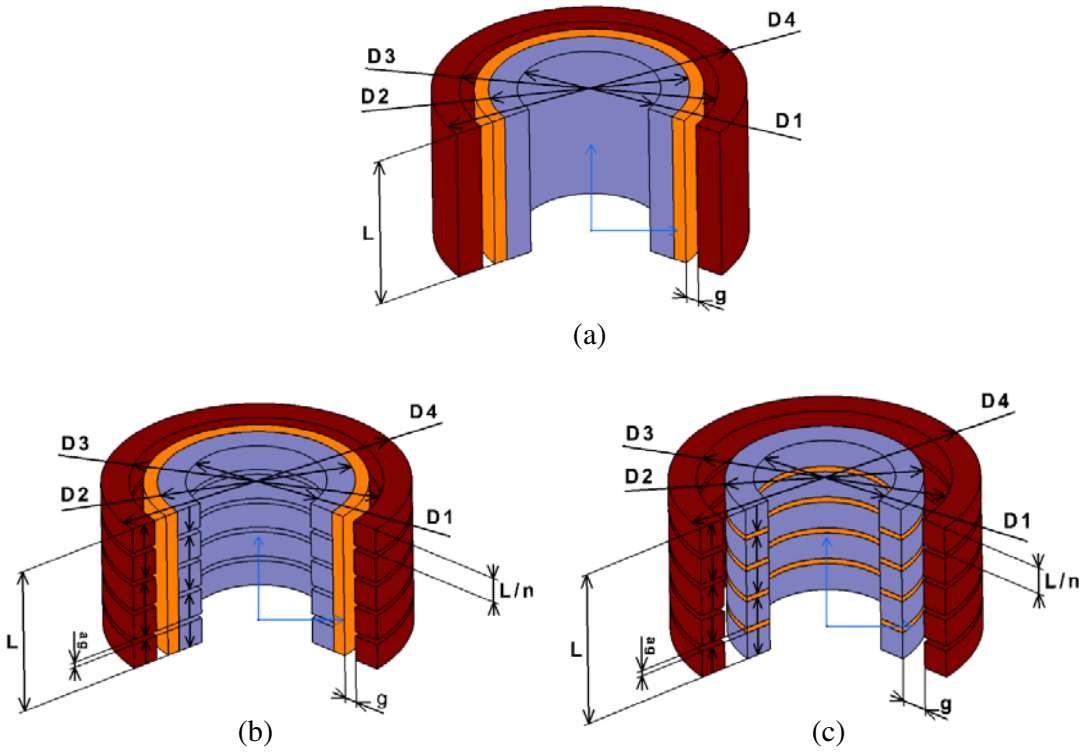

Figure 1. Magnetic bearing configurations with ECD, (a) monolithic with copper plate on rotor ring, (b) MPMTB with a copper plate on the rotor rings, and (c) MPMTB with copper rings between axial stacks.

3. OPTIMIZATION OF PERMANENT MAGNET THRUST BEARING

Two approaches are used to optimize the parameters of MPMTB for optimum characteristics: minimizing the magnet volume for achieving the required magnitudes of force and stiffness and second; maximizing bearing features in a particular volume of the magnet. The magnetic interactions between the rotor and stator rings in MPMTB are shown in Fig. 2, and a generalized equation of force is given in Eq. (1).

$$F_Z = \frac{B_r^2}{4\pi\mu_0} \sum_{u=1}^{n} \sum_{v=1}^{n} \sum_{k=1}^{2} \sum_{l=3}^{4} \sum_{p=1}^{m} \sum_{q=1}^{m} \frac{S_{pku}\, S_{qlv}}{R^3_{(pku)(qlv)}} \mathbf{R_{(pku)(qlv)}} (-1)^{(k+l)} (-1)^{(u+v)} \tag{1}$$

where $\mathbf{R_{(pku)(qlv)}} = (X_{qlv} - X_{pku})\mathbf{i} + (Y_{qlv} - Y_{pku})\mathbf{j} + (Z_{qlv} - Z_{pku})\mathbf{k}$ is the position vector, and equations for coordinates of elements considered on the end faces of magnets are,

$$\begin{aligned}
(X_{pku})_{1,2} &= (x + r_{mr}\cos\beta)\mathbf{i} & (X_{qlv})_{3,4} &= (r_{ms}\cos\alpha)\mathbf{i} \\
(Y_{pku})_{1,2} &= (y + r_{mr}\sin\beta)\mathbf{j} & (Y_{qlv})_{3,4} &= (r_{ms}\sin\alpha)\mathbf{j} \\
(Z_{pku})_{1} &= (z + (u-1)\,l + (u-1)\,ag)\mathbf{k} & (Z_{qlv})_{\mathbf{3}} &= ((v-1)l + (v-1)\,ag)\,\mathbf{k} \\
(Z_{pku})_{2} &= (z + (u)\,l + (u-1)\,ag)\mathbf{k} & (Z_{qlv})_{\mathbf{4}} &= (vl + (v-1)\,ag)\,\mathbf{k}
\end{aligned}$$

Suffixes 1, 2 and 3, 4 are the end faces of rotor and stator rings. For the detailed explanation of different notations, readers are suggested to refer [17].

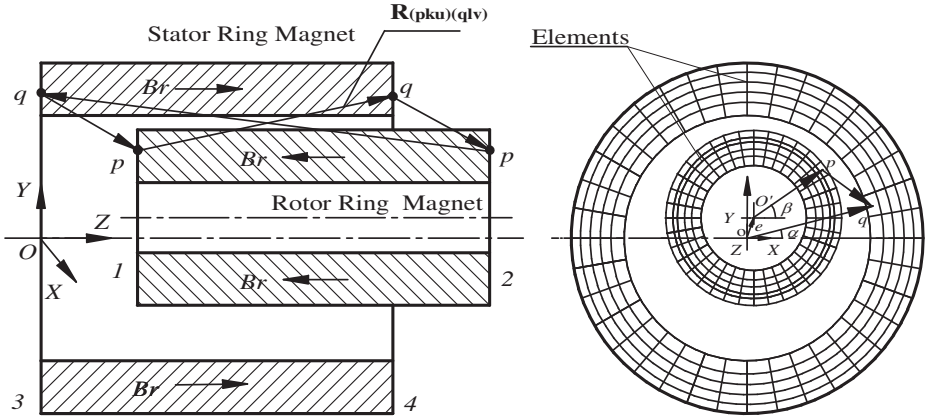

Figure 2. Interaction between stator and rotor rings of MPMTB.

The detailed design methodology for optimizing the bearing parameters and maximizing the characteristics of MPMTB was presented in [29] by our research team. In the present work, PMB is optimized by following the steps given below, and calculated values are presented in Table 1.

1. Selection of ratios ($g/D4$ & $L/D4$) among the specified values:
   Ratios describe available space around the shaft in a particular application. In the present work, $g/D4 = 0.02$ and $L/D4$ (aspect ratio) $= 1$ are chosen.
2. Selection of air gap:
   The air gap value (g) is to be selected based on force and stiffness requirements and the availability of sizes of magnet rings. Arbitrarily, $g = 2\,\text{mm}$ is taken, and $D4 = 100\,\text{mm}$ and $L = 100$ are calculated.
3. Calculation of optimum design variables (n, ag, $D1$, $D2$, and $D3$) of the bearing for maximum axial force:
   Variables are calculated using the corresponding curve fit equations, and results are shown in Table 1.

Table 1. Optimized bearing dimensions for maximum Fz.

For, $g/D4 = 0.02$ and $L/D4 = 1$, Let $g = 2\,\text{mm} \Longrightarrow D4 = 100\,\text{mm}$; $L = 100\,\text{mm}$	
Optimum Parameters	**Values**
Number of magnet rings (n)	7
Air gap between adjacent rings (ag)	5.66 mm
Inside diameter of rotor rings ($D1$)	3* mm
Outside diameter of rotor rings ($D2$)	70.08 mm
Inside diameter of stator rings ($D3$)	74.08 mm
Ratio of maximized axial force of optimized bearing and axial force of single ring bearing (Fz/Fzs)	9.6
Axial force of single ring bearing (Fzs)	951.9 N
Maximized force calculated using proposed optimization methodology (Fzp)	9138.24 N
Maximized force calculated using math. model (Fzc)	8951 N
Maximized force calculated using FEA in Ansys (Fza)	8823 N

* $D1 = 10\,\text{mm}$ is taken for providing strength to the shaft

4. Calculation of the ratio of maximized axial force of MPMTB and monolithic bearing (Fz/Fzs):
   The ratio is evaluated using the corresponding curve fit equation, and the value is given in Table 1.
5. Calculation of force in monolithic bearing configuration (Fzs):
   Force is calculated from Eq. (1).
6. Calculation of the maximized force of the optimized MPMTB (Fz):
   Maximized force is obtained by referring to the ratio evaluated in step 4.

In addition, the axial force of MPMTB is evaluated by solving complicated Eq. (1) in MATLAB for optimized values of the design variables, and results are graphed in Fig. 3(a) along with results of monolithic bearing configuration. The maximized value of force using proposed optimization methodology and calculated using the presented mathematical model (Eq. (1)) match closely, and a deviation of 2.05% is observed among force values. The axial force results of the optimized bearing are also calculated using 3D FEA in ANSYS at different axial displacements of the rotor with stator, and the values are depicted in Fig. 3(b) along with results of a mathematical model. Results match closely, and a deviation of 1.27% is observed.

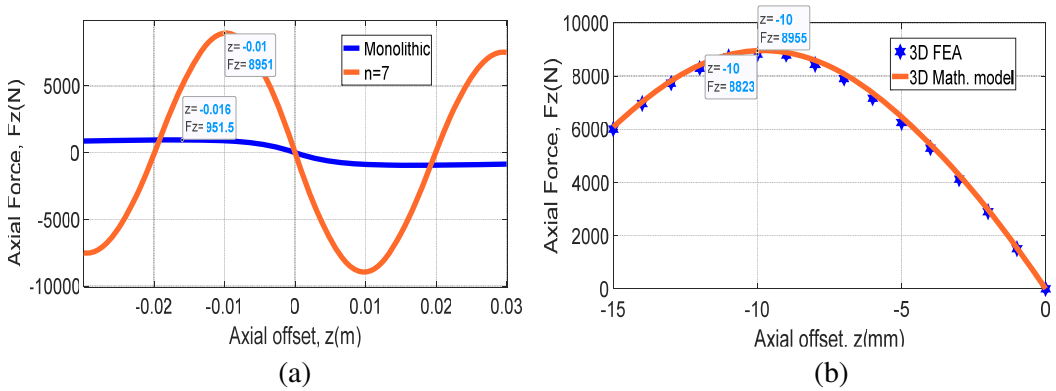

Figure 3. Results of optimized MPMTB. (a) Axial force comparison. (b) Results of 3D FEA and mathematical model.

4. ANALYSIS OF EDDY CURRENT DAMPERS

In the present work, 3D electromagnetic transient analysis is used to analyze the proposed configurations of ECD for force and damping coefficients. This analysis is carried out in ANSYS using 3D FEA. To form an ECD in configuration I, a cylindrical copper plate is taken on the surface of rotor rings of the optimized MPMTB. In configuration II, copper rings are provided in an axial air gap between adjacent magnet rings of the same optimized MPMTB to generate an eddy current damping effect. Two bearing geometries are modeled in Ansys with a maximum of 405494 SOLID97 elements, and permanent magnet rings are polarized in the axial directions by providing coercive forces. Rotor rings are positioned at an axial distance of -10 mm with the stator rings in both configurations to achieve maximum axial force value. The dimension values and material properties of MPMTB and ECD are given in Table 2.

Table 2. Material properties of MPMTB and ECD.

S. No.	Material	Relative Permeability	Resistivity (Ω.m)	Dimensions
1	N48 grade, NdFeB Magnet rings ($B_r = 1.2$ T)	1.043	1.8×10^{-6}	$D1 = 10$ mm, $D2 = 70.08$ mm, $D3 = 74.08$ mm, $D4 = 100$ mm, $n = 7$ (on rotor and stator)
2	Copper plate	1	1.72×10^{-8}	Thickness, $t = 1$ mm, and axial length, $l = 131.96$ mm
3	Copper rings	1	1.72×10^{-8}	Number of rings = 6, $D1 = 10$ mm, $D2 = 70.08$ mm and axial length of each ring = ag = 5.66 mm
4	Air	1	–	–

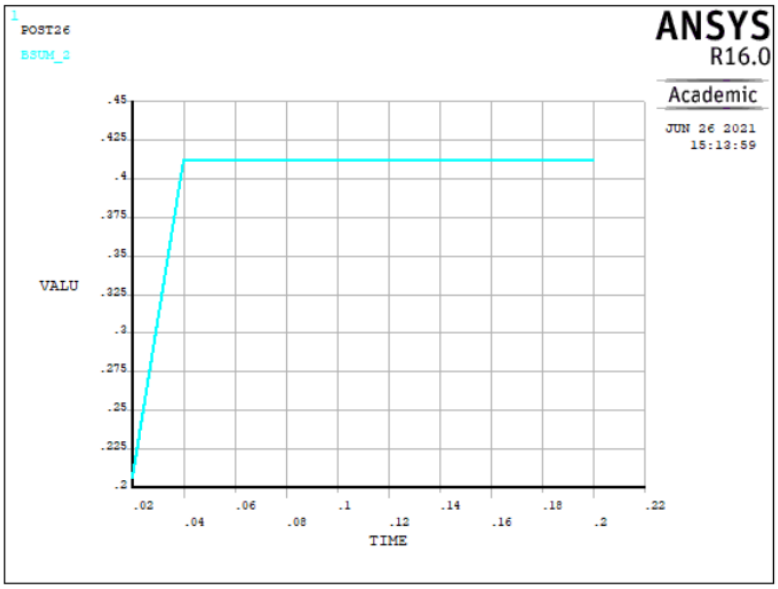

Figure 4. Magnetic flux density vs time.

The rotor rotation induces an eddy current in the conductor plate, and Lorentz force is exerted on the copper plate due to interaction between induced current and the magnetic field. In transient analysis, a stable magnetic field of permanent magnets is generally obtained by two-step loading as shown in Fig. 4. In the first step, the magnetic field increases to the maximum value, and it remains constant with time in the second loading step. In this analysis, the automatic time stepping and time integration effect is kept.

Finite element transient analysis is carried out for axial and radial speeds of the rotor in a bearing. The speeds are varied from 0 to 100 m/s in steps of 10 m/s. Eddy current distributions in the conductor plate of configuration I and in the copper rings of the rotor in configuration II are shown in Figs. 5 and 6.

The calculated values of axial damping force with axial velocity and radial damping force with a

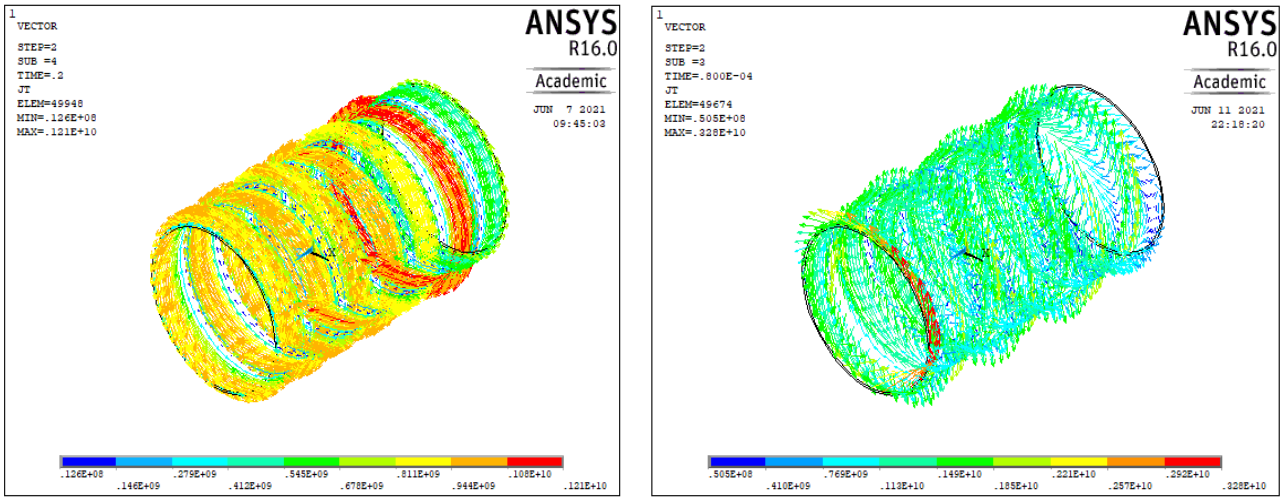

(a) (b)

Figure 5. Eddy current distribution in copper plate of configuration I at, (a) axial speed of 30 m/s, (b) radial speed of 100 m/s of rotor.

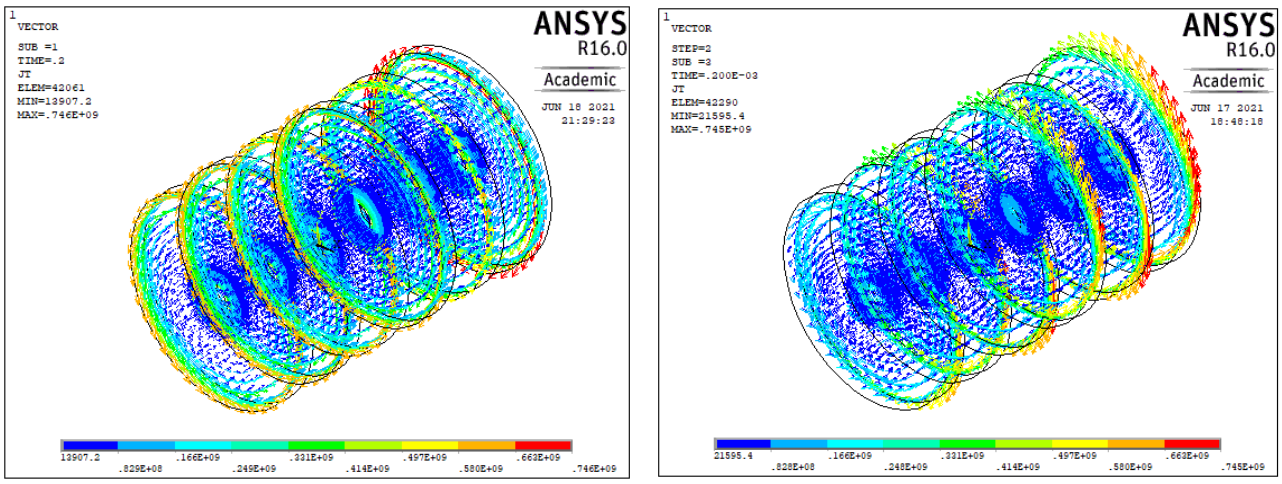

(a) (b)

Figure 6. Eddy current distribution in copper rings of configuration II at (a) axial speed of 10 m/s, (b) radial speed of 10 m/s of rotor.

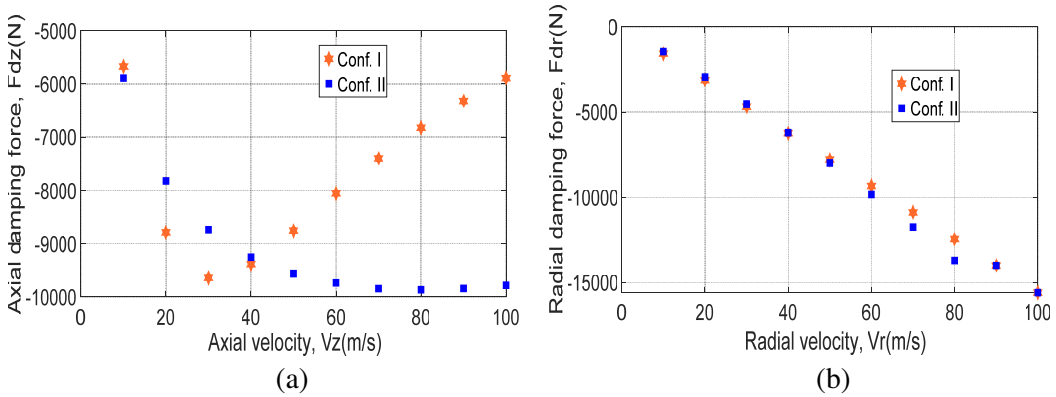

Figure 7. Results of damping force in configurations I & II, (a) axial damping force vs axial velocity of the rotor, (b) radial damping force vs radial velocity of the rotor.

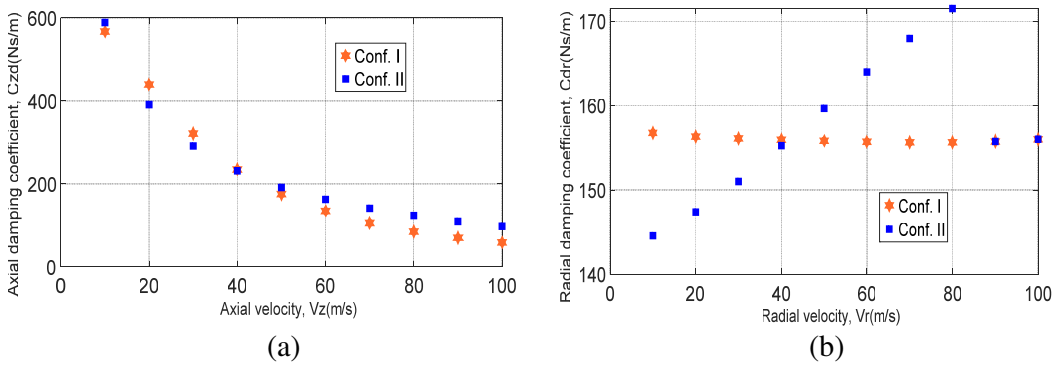

Figure 8. Results of damping coefficient in configurations I & II, (a) axial damping coefficient vs axial velocity of the rotor, (b) radial damping coefficient vs radial velocity of the rotor.

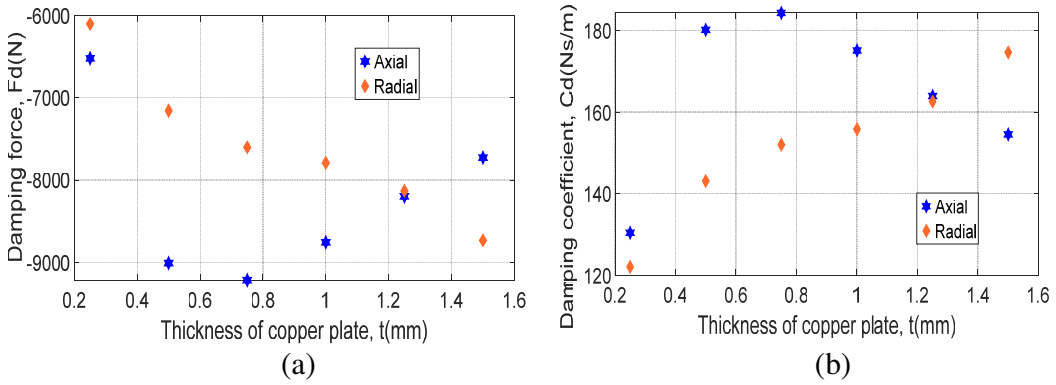

Figure 9. Results of configuration I at 50 m/s velocity of the rotor, (a) axial and radial damping forces, (b) axial and radial damping coefficients.

radial velocity of the rotor for both configurations are plotted in Fig. 7. The axial damping force increases with axial velocity and reaches a maximum at 30 m/s, and decreases thereafter in configuration I, whereas in configuration II, it increases to a maximum value and becomes almost constant with an increase in the axial velocity of the rotor. The maximum axial damping force (9863.45 N at 80 m/s) generated in configuration II is slightly higher than configuration I (9638.26 N at 30 m/s). The radial

damping force increases with the radial velocity of the rotor in both configurations, and force values of configuration I are slightly higher than configuration II up to 40 m/s, and thereafter slightly higher values of the force are observed in configuration II than I. Axial and radial damping coefficients are evaluated at different velocities in both configurations and are plotted in Fig. 8. Axial damping coefficient decreases with an increase in the velocity of the rotor in both the configurations, and the radial damping coefficient is almost constant (∼156 Ns/m) in configuration I, whereas in configuration II it fluctuates from 144 to 171 Ns/m.

Damping forces and coefficients are calculated for different thicknesses of copper plate in the configuration I at 50 m/s axial and radial velocity of the rotor. The results shown in Fig. 9 indicate that the axial damping force and coefficient increase with the thickness of the plate and reach optimum at 0.75 mm, and then decrease, whereas radial damping force and coefficient increase with the thickness of the copper plate.

5. CONCLUSIONS

In this paper, novel and conventional eddy current dampers are analyzed for damping forces and coefficients for an optimized MPMTB. The following are the conclusions based on the analysis of the present work:

- Optimization of PMTB is carried out by selecting a particular volume of magnet (three general parameters, i.e., $g/D4 = 0.02$, $g = 2$ mm and $L/D4 = 1$) with the help of proposed optimization methodology.
- The value of force in an optimized MPMTB is 9.6 times the value of the monolithic bearing configuration.
- The maximum axial damping force generated in the novel structure is slightly higher than the conventional structure for 1 mm thickness of the copper plate.
- The axial and radial damping forces developed in the configuration I are dependent on the thickness of the copper plate. Axial damping force is maximum (9215.1 N) at 0.75 mm thickness for 50 m/s axial velocity of the rotor. The radial damping force increases with the thickness of the copper plate for 50 m/s radial velocity of the rotor.

ACKNOWLEDGMENT

Authors acknowledge the support provided by Manipal Institute of Technology, Manipal Academy of Higher Education, Manipal and ME Department of National Institute of Technology Karnataka, Surathkal for carrying out the research work.

REFERENCES

1. Yonnet, J. P., "Passive magnetic bearings with permanent magnets," *IEEE Trans. Magn.*, Vol. 14, No. 5, 803–805, 1978.
2. Schweitzer, G., "Magnetic bearings-applications, concepts and theory," *JSME International Journal Series III*, Vol. 33, No. 1, 13–18, 1990.
3. Sotelo, G. G., R. Andrade, and A. C. Ferreira, "Magnetic bearing sets for a flywheel system," *IEEE Trans. on Applied Super Conductivity*, Vol. 17, No. 2, 2150–2153, 2007.
4. Le, Y., J. Fang, and J. Sun, "Design of a Halbach array permanent magnet damping system for high speed compressor with large thrust load," *IEEE Trans. Magn.*, Vol. 51, No. 1, 1–9, 2015.
5. Mukhopadhaya, S. C., et al., "Fabrication of a repulsive-type magnetic bearing using a novel arrangement of permanent magnets for vertical-rotor suspension," *IEEE Trans. Magn.*, Vol. 39, 3220–3222, 2003.
6. Bekinal, S. I., S. Jana, and S. S. Kulkarni, "A hybrid (permanent magnet and foil) bearing set for complete passive levitation of high-speed rotors," *Proc. IMechE, Part C: J. Mechanical Engineering Science*, Vol. 231, 3679–3689, 2017.

7. Bekinal, S. I., T. R. Anil, and S. Jana, "Analysis of axially magnetized permanent magnet bearing characteristics," *Progress In Electromagnetics Research B*, Vol. 44, 327–343, 2012.
8. Ravaud, R., G. Lemarquand, and V. Lemarquand, "Force and stiffness of passive magnetic bearings using permanent magnets. Part 1: Axial magnetization," *IEEE Trans. Magn.*, Vol. 45, No. 7, 2996–3002, 2009.
9. Ravaud, R., G. Lemarquand, and V. Lemarquand, "Force and stiffness of passive magnetic bearings using permanent magnets. Part 2: Radial magnetization," *IEEE Trans. Magn.*, Vol. 45, No. 9, 3334–3342, 2009.
10. Bekinal, S. I., A. T. Ramakrishna, and S. Jana, "Analysis of radial magnetized permanent magnet bearing characteristics," *Progress In Electromagnetics Research B*, Vol. 47, 87–105, 2013.
11. Bekinal, S. I., A. T. Ramakrishna, and S. Jana, "Analysis of radial magnetized permanent magnet bearing characteristics for five degrees of freedom," *Progress In Electromagnetics Research B*, Vol. 52, 307–326, 2013.
12. Samanta, P. and H. Hirani, "Magnetic bearing configurations: Theoretical and experimental studies," *IEEE Trans. Magn.*, Vol. 44, No. 2, 292–300, 2008.
13. Tian, L. L., X. P. Ai, and Y. Q. Tian, "Analytical model of magnetic force for axial stack permanent-magnet bearings," *IEEE Trans. Magn.*, Vol. 48, No. 10, 2592–2599, 2012.
14. Marth, E., G. Jungmayr, and W. Amrhein, "A 2-D-based analytical method for calculating permanent magnetic ring bearings with arbitrary magnetisation and its application to optimal bearing design," *IEEE Trans. Magn.*, Vol. 50, No. 5, 1–8, 2014.
15. Bekinal, S. I., M. Doddamani, and N. D. Dravid, "Utilization of low computational cost two dimensional analytical equations in optimization of multi rings permanent magnet thrust bearings," *Progress In Electromagnetics Research M*, Vol. 62, 51–63, 2017.
16. Bekinal, S. I. and S. Jana, "Generalized three-dimensional mathematical models for force and stiffness in axially, radially, and perpendicularly magnetized passive magnetic bearings with 'n' number of ring pairs," *ASME Journal of Tribology*, Vol. 138, No. 3, 031105(1–9). 2016.
17. Bekinal, S. I., M. R. Doddamani, and S. Jana, " Optimization of axially magnetized stack structured permanent magnet thrust bearing using three dimensional mathematical model," *ASME Journal of Tribology*, Vol. 139, No. 3, 031101(1–9), 2017.
18. Bekinal, S. I., M. R. Doddamani, B. V. Mohan, and S. Jana, "Generalized optimization procedure for rotational magnetized direction permanent magnet thrust bearing configuration," *Proc. IMechE, Part C: J. Mechanical Engineering Science*, Vol. 233, 2563–2573, 2019.
19. Lijesh, K. P., M. R. Doddamani, and S. I. Bekinal, "A pragmatic optimization of axial stack-radial passive magnetic bearings," *ASME Journal of Tribology*, Vol. 140, 021901(1–9), 2018.
20. Lijesh, K. P., M. R. Doddamani, S. I. Bekinal, and S. M. Muzakkir, "Multi-objective optimization of stacked radial passive magnetic bearing," *Proc. IMechE, Part J: J. Engineering Tribology*, Vol. 232, 1140–1159, 2018.
21. Sodano, H. A. and D. J. Inman, "Modeling of a new active eddy current vibration control system," *ASME Journal of Dynamic Systems, Measurement and Control*, Vol. 130, 021009-1–11. 2008.
22. Passenbrunner, J., G. Jungmayr, and W. Amrhein, "Design and analysis of a 1D actively stabilized system with viscoelastic damping support," *Actuators*, Vol. 8, No. 33, 2–18, 2019
23. Cheah, S. K. and H. A. Sodano, "Novel eddy current damping mechanism for passive magnetic bearings," *Journal of Vibration and Control*, Vol. 14, No. 11, 1749–1766, 2008.
24. Fang, J., Y. Le, J. Sun, and K. Wang, "Analysis and design of passive magnetic bearing and damping system for high-speed compressor," *IEEE Trans. Magn.*, Vol. 48, No. 9, 2528–2537, 2012.
25. Detoni, J. G., Q. Cui, N. Amati, and A. Tonoli, "Modelling and evaluation of damping coefficient of eddy current dampers in rotordynamic applications," *Journal of Sound and Vibration*, Vol. 373, 52–65, 2016.
26. Safaeian, R. and H. Heydari, "Optimal design of a compact passive magnetic bearing based on dynamic modelling," *IET Electric Power Applications*, Vol. 13, No. 6, 720–729, 2019.

27. Safaeian, R. and H. Heydari, "Comprehensive comparison of different structures of passive permanent magnet bearings," *IET Electric Power Applications*, Vol. 12, No. 2, 179–187. 2017.
28. Bekinal, S. I. and M. Doddamani, "Improvement in the design calculations of multi ring permanent magnet thrust bearing," *Progress In Electromagnetics Research M*, Vol. 94, 83–93, 2020.
29. Bekinal, S. I. and M. Doddamani, "Optimum design methodology for axially polarized multi-ring radial and thrust permanent magnet bearings," *Progress In Electromagnetics Research B*, Vol. 88, 197–215, 2020.